Deviations from Boltzmann-Gibbs Statistics in Confined Optical Lattices

Andreas Dechant,[1,2] David A. Kessler,[1] and Eli Barkai[1]
[1]Department of Physics, Bar Ilan University, Ramat-Gan 52900, Israel
[2]Department of Physics, Friedrich-Alexander-Universität Erlangen-Nürnberg, 91058 Erlangen, Germany
(Received 19 December 2014; published 23 October 2015)

We investigate the semiclassical phase-space probability distribution $P(x, p)$ of cold atoms in a Sisyphus cooling lattice with an additional harmonic confinement. We pose the question of whether this nonequilibrium steady state satisfies the equivalence of energy and probability. This equivalence is the foundation of Boltzmann-Gibbs and generalized thermostatic statistics, and a prerequisite for the description in terms of a temperature. At large energies, $P(x, p)$ depends only on the Hamiltonian $H(x, p)$ and the answer to the question is yes. In distinction to the Boltzmann-Gibbs state, the large-energy tails are power laws $P(x, p) \propto H(x, p)^{-1/D}$, where D is related to the depth of the optical lattice. At intermediate energies, however, $P(x, p)$ cannot be expressed as a function of the Hamiltonian and the equivalence between energy and probability breaks down. As a consequence the average potential and kinetic energy differ and no well-defined temperature can be assigned. The Boltzmann-Gibbs state is regained only in the limit of deep optical lattices. For strong confinement relative to the damping, we derive an explicit expression for the stationary phase-space distribution.

DOI: 10.1103/PhysRevLett.115.173006 PACS numbers: 37.10.Jk, 05.10.Gg

The search for generalized forms of Boltzmann-Gibbs (BG) statistics, especially those related to fractal and power-law concepts, has attracted considerable interest [1–4]. Among this class of systems, laser cooled atoms in optical lattices are especially appealing. Here, the light field replaces the classical heat bath of temperature T and we are generally not in thermal equilibrium, raising the question of what replaces the canonical BG distribution and how the statistical description changes. The excellent tunability of optical lattices allows us to perform state engineering. In the case of driven dissipative systems the dissipation can be tuned to guide the system towards a desired nonequilibrium steady state [5–7]. The dissipation mechanism in conjunction with excitation of the atoms by the light field also governs the statistics of subrecoil laser cooling and Sisyphus cooling, both recognized to yield power-law statistics and deviations from the standard equilibrium framework [3,8–14]. Since these cooling techniques are used in laboratories all over the world, the generalization of standard statistical mechanics becomes a very practical problem. In Sisyphus cooling, the nonlinear momentum dependence of the cooling mechanism, discussed in more detail below, induces a wealth of unusual and interesting statistical effects; for a recent review see Ref. [4]. In particular, the velocity distribution of the cold atoms was predicted and later shown experimentally to follow Tsallis statistics [12,15], contrary to the Gaussian BG statistics found in linearly damped systems. The insight that power-law statistics describe a broad range of systems in physics [16–18] warrants a second, closer look at cold atoms as an experimental toolbox to explore the novel steady-state statistics of these nonequilibrium systems.

In this Letter, we investigate a semiclassical model of atoms in an optical lattice with an additional confining field and discuss the resulting nonequilibrium stationary phase-space probability distribution function (PSPDF). In particular, we focus on the question of how this PSPDF differs from BG or Tsallis statistics. Both BG and Tsallis statistics are based on the approach of thermostatics [1,19], i.e., the minimization of an entropy functional under the constraint of constant mean energy. A natural consequence of this approach is energy equipartition [19]; states with the same energy occur with the same probability and the PSPDF is a function of the system's Hamiltonian. Without a confining potential, the atomic cloud spreads diffusively or even superdiffusively [10,11,14,20–22], and thus there is no stationary PSPDF. For the momentum distribution, the equivalence between energy and probability is realized trivially, as the momentum is the only degree of freedom entering the Hamiltonian $H = p^2/(2m)$. The stationary momentum distribution when written as a function of the Hamiltonian turns out to be of the Tsallis form [12,15]. By adding a confining potential, the position of the atoms enters the Hamiltonian as a second degree of freedom. Only then the connection between the PSPDF and the Hamiltonian can potentially be nontrivial. The main questions we wish to answer in the following are as follows. Under what conditions is the PSPDF solely a function of the Hamiltonian? If this is the case, then are the statistics described by BG or Tsallis statistics? And if not, how does the PSPDF deviate from the latter and what are the consequences? The answers to these questions reveal rich physical phenomena and depend on the parameters of the lattice and the confining field, as well as the energy scale.

Model.—Within the semiclassical description, the atoms are subject to a nonlinear, momentum-dependent friction force, which encapsulates the cooling mechanism [9]. In addition, there are random recoil events due to the spontaneous emission of photons, modeled as Gaussian white noise $\langle \eta(t)\eta(t')\rangle = 2D_p\delta(t-t')$. The atoms' dynamics is described by the Langevin equation [9,10]

$$\dot{x}(t) = \frac{p(t)}{m},$$
$$\dot{p}(t) = \underbrace{-\gamma \frac{p(t)}{1+p^2(t)/p_c^2}}_{\text{friction force}} \underbrace{-U'[x(t)]}_{\text{confinement}} \underbrace{+\eta(t)}_{\text{noise}}, \qquad (1)$$

where γ is the damping coefficient, p_c is the capture momentum, and D_p is the momentum diffusion coefficient [23], which can be expressed in terms of the optical lattice parameters. We restrict our discussion to the one-dimensional case, which has been realized in several experiments [10,11,14,24]. In addition, the particles are subject to an external confining potential, which we take to be harmonic, $U(x) = m\omega^2 x^2/2$. Higher-dimensional Sisyphus cooling can lead to spatial inhomogeneity [25] and we want to avoid this complication here. At small momenta $|p| \ll p_c$, the friction force is Stokes-like, $F_f(p) \propto -p$, i.e., linear in the momentum. For entirely linear friction, we would obtain precisely the BG distribution with $k_B T = D_p/(\gamma m)$ for the stationary state of the system. However, at large momenta $|p| \gg p_c$ the magnitude of the friction force decreases as $F_f(p) \propto -1/p$ with momentum—the cooling mechanism fails for very fast atoms. This nonlinearity of the friction force induces temporal correlations in the motion of the atoms [10], as fast atoms experience only a weak friction force and thus tend to stay fast. These correlations in the absence of a confining potential are responsible for the power-law statistics and anomalous dynamics [22,26]. The stationary PSPDF of the ensemble of random motions described by Eq. (1) is given by the Klein-Kramers equation [27]. For convenience of notation, we switch to dimensionless variables $m\omega x/p_c \to x$, $p/p_c \to p$

$$\left[\Omega[x\partial_p - p\partial_x] + \partial_p\left[\frac{p}{1+p^2} + D\partial_p\right]\right]P(x,p) = 0. \qquad (2)$$

We here defined the dimensionless parameters $\Omega = \omega/\gamma$, quantifying the strength of the confining potential, and $D = D_p/(\gamma p_c^2)$, related to the depth of the optical lattice U_0 by $D = cE_r/U_0$ with the photon recoil energy E_r and a constant $c \sim \mathcal{O}(10)$ that depends on the details of the experimental system [10,13]. Note that in the following, we always consider the case $D < 1$, since only here a stationary state exists; the case $D > 1$ will be discussed elsewhere [28].

Strong confinement $\Omega \gg 1$.—We expect the system to be accurately described by its energy whenever its evolution is approximately Hamiltonian, i.e., when dissipation and noise can be treated as small perturbations. More precisely, this underdamped limit [29–31] is defined by the condition that the change in energy over one period of the Hamiltonian evolution is small compared to the total energy. We can formalize this by introducing the energy $E = (p^2+x^2)/2$ and the phase-space angle $\alpha = \arctan(p/x)$ in terms of which Eq. (2) reads

$$[\partial_\alpha + \Omega^{-1}\mathcal{L}_E]P(E,\alpha) = 0 \quad \text{with}$$
$$\mathcal{L}_E = \partial_\alpha \frac{\sin(\alpha)\cos(\alpha)}{1+2E\sin^2(\alpha)} + \partial_E \frac{2E\sin^2(\alpha)}{1+2E\sin^2(\alpha)}$$
$$+ D\left[2\partial_\alpha \sin(\alpha)\cos(\alpha)\partial_E + \frac{1}{2E}\partial_\alpha \cos^2(\alpha)\partial_\alpha + [\sin^2(\alpha) - \cos^2(\alpha)]\partial_E + 2\sin^2(\alpha)\partial_E E\partial_E\right]. \qquad (3)$$

Here, the operator $\mathcal{L}_E$ contains the terms due to friction and noise, while the operator ∂_α describes the Hamiltonian dynamics. Obviously, the underdamped approximation holds for $\Omega \gg 1$, where we have to leading order $\partial_\alpha P(E,\alpha) = 0$ and thus

$$P(E,\alpha) \simeq P_E(E)/(2\pi) + \mathcal{O}(\Omega^{-1}). \qquad (4)$$

Plugging this into Eq. (3) and integrating over α, we find an equation for the stationary energy probability distribution function (PDF)

$$\left[\partial_E\left(1 - \frac{1}{\sqrt{1+2E}}\right) + D\partial_E E\partial_E\right]P_E(E) = 0. \qquad (5)$$

The normalized solution to this stationary energy-diffusion equation reads, for $D < 1$,

$$P_E(E) = \frac{2^{2/D}(1-D)(2-D)}{2D}(1+\sqrt{1+2E})^{-2/D}. \qquad (6)$$

Changing back to position and momentum, we obtain to leading order a PSPDF $P(x,p) = P_E(H(x,p))/(2\pi)$ that depends only on the Hamiltonian. Contrary to the BG density, however, the distribution is not exponential in the Hamiltonian, and does not factorize into a potential and kinetic part. The energy PDF (6) is compared to the results from numerical simulations in Fig. 1 and shows excellent agreement with the latter already for moderate values of the frequency. Asymptotically for large energies, the energy

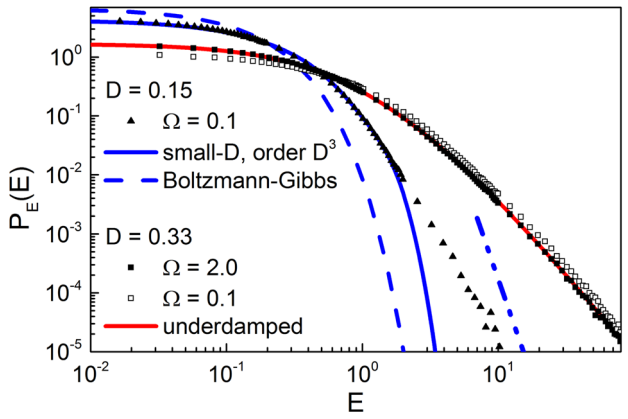

FIG. 1 (color online). Energy PDFs for $D = 1/3$ and $D = 3/20$. Symbols are data from numerical simulations of Eq. (1); colored lines are analytical results. For the larger value of $D = 1/3$ (red, squares), the underdamped approximation (6) is accurate even for moderate frequencies $\Omega = 2.0$ (full squares). For small frequencies $\Omega = 0.1$ (empty squares), the energy PDF differs in the center; the tails, however, still follow the same power-law behavior $P_E(E) \propto E^{-1/D}$. For smaller values of D (blue, triangles), the PDF has more weight in the center and is there described by the small-D expansion (12) (full line), which considerably improves upon the naive BG distribution (dashed line). The large energy power law (dash-dotted line) is approached very slowly.

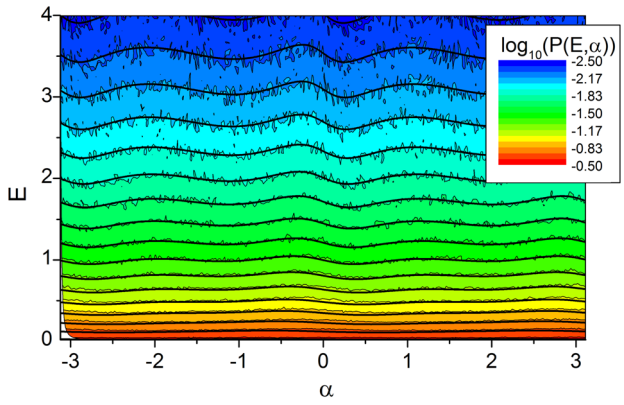

FIG. 2 (color online). PSPDF for $D = 1/3$ and $\Omega = 2$ as a function of energy E and angle α. The colored areas are the result of numerical Langevin simulations; the bold contours are the analytical results from the underdamped approximation (8) up to order Ω^{-1}. While for small energies the equiprobability lines are approximately straight lines, for intermediate energies the angle dependence is clearly visible.

PDF (6) behaves as a power law $P_E(E) \propto E^{-1/D}$. The momentum PDF decays as $P_p(p) \propto p^{-2/D+1}$ for large momenta, which is markedly different from the exponent $P_p(p) \propto p^{-1/D}$ obtained without the confinement [9]. The power-law form of the energy PDF immediately implies that the average energy

$$\langle E \rangle = \frac{D(2-D)}{(2-3D)(1-2D)} \tag{7}$$

diverges in the stationary state for $D > 1/2$, where it increases as a function of time and a time-dependent description is needed to obtain the average energy. Importantly, the average kinetic energy $\langle E_k \rangle = \langle E \rangle/2$ is always smaller than the result of Ref. [9] found for the unconfined system. This implies that the confinement increases the effectiveness of the friction mechanism: fast particles, for which the friction force tends to zero [see Eq. (1)], eventually decelerate due to the harmonic restoring force and reenter the momentum range where the friction is sizable, thus increasing overall dissipation. The energy PDF (6) is the leading order of an expansion in terms of Ω^{-1} [32]. More precisely, we have

$$P(E,\alpha) = \frac{P_E(E)}{2\pi}\left[1 + \frac{f_1(E,\alpha)}{\Omega} + \mathcal{O}(\Omega^{-2})\right], \tag{8}$$

which allows us to find corrections for finite frequencies. These correction terms, derived in the Supplemental Material [33], depend on the angle α and thus violate energy equipartition. The PSPDF corresponding to this first-order result is shown in Fig. 2. Except at low energies, this exhibits clear deviations from equiprobable energy surfaces, which would appear as straight lines, and shows excellent agreement between our theory and simulation results. Equation (6) tends to the BG distribution in the limit $D \to 0$, which is reminiscent of the Tsallis q exponential [1] found for the free case [12,15]. However, even though the PSPDF is a function of the Hamiltonian in the limit of large Ω, it is clearly not a q exponential, which implies that Tsallis statistics do not provide the general solution for this system.

Large energies $E \gg 1$.—Importantly, the asymptotic behavior $P_E(E) \propto E^{-1/D}$ (6) is not only valid for large Ω, but is the generic case for large energies. Physically, this is due to the nonlinear behavior of the friction force, which tends to zero for large momenta and thus leads to underdamped behavior at large energies. The large energy tails of the PSPDF are thus universally described by the underdamped approximation and are a function of the Hamiltonian only. This can be understood by noting that, except in a small "strip" around $\alpha = 0$ and $\pm\pi$, where $E\sin^2(\alpha)$ is small, the operator $\mathcal{L}_E$ in Eq. (3) is of order E^{-1}. Similar to Eq. (8), we can expand the PSPDF

$$P(E,\alpha) \simeq \frac{P_E(E)}{2\pi}\left[1 + \frac{g_1(\alpha)}{E} + \mathcal{O}(E^{-2})\right]. \tag{9}$$

Expanding $\mathcal{L}_E$ for large energies, we can determine the function $g_1(\alpha)$ (see the Supplemental Material [33]). The resulting asymptotic PSPDF up to order E^{-1} reads

$$P(E,\alpha) \simeq NE^{-(1/D)}\left[1 - \frac{\sqrt{2}}{D}E^{-1/2} + \frac{1}{D^2}E^{-1} + \left[\frac{1}{2\Omega}\left(\left(1+\frac{1}{D}\right)\sin(2\alpha) - \cot(2\alpha)\right)\right]E^{-1}\right], \tag{10}$$

where N is a normalization constant. The first three terms on the right-hand side stem from the large energy expansion of $P_E(E)$, whereas the remaining term is the angle-dependent correction $g_1(\alpha)$. Equation (10) diverges at $\alpha = 0$ and $\pm\pi$. These singularities occur because in Eq. (10) we expanded for large E, assuming that $2E\sin^2(\alpha)$ is large, which breaks down in the strip. Inside the strip, we express Eq. (3) as a function of $z = \sqrt{2E}\alpha$ and E and again expand for large energies. Careful asymptotic matching of both expansions and the condition that $P(E, \alpha)$ is a periodic function of α fixes any occurring integration constants. We will detail this procedure in a longer publication [28]; the result up to order E^{-1} is given in Eq. (S12) in the Supplemental Material [33]. The main conclusion from Eq. (9) is that, for large energies, the PSPDF decays as a power law in energy, with small angle-dependent corrections.

Deep lattices $D \ll 1$.—For small D, the atoms are typically slow and thus the friction is approximately linear. While the large energy tails are still given by Eq. (9), the power law decays very fast for small D and the center part dominates the statistics. In this regime, we thus expect the BG equilibrium distribution to approximate the PSPDF. Indeed, by rescaling $\tilde{x} = x/\sqrt{D}$ and $\tilde{p} = p/\sqrt{D}$ in Eq. (2), we see that in the limit $D \to 0$, we recover the usual Stokes friction result and thus the BG distribution $P_{\mathrm{BG}}(\tilde{x}, \tilde{p}) \propto e^{-(\tilde{p}^2+\tilde{x}^2)/2}$. We define an auxiliary function $h(\tilde{x}, \tilde{p})$ via $P(\tilde{x}, \tilde{p}) = P_{\mathrm{BG}}(\tilde{x}, \tilde{p})h(\tilde{x}, \tilde{p})$ and expand the latter with respect to D

$$h(\tilde{x}, \tilde{p}) \simeq 1 + Dh_1(\tilde{x}, \tilde{p}) + D^2h_2(\tilde{x}, \tilde{p}) + \mathcal{O}(D^3). \tag{11}$$

Plugging this into Eq. (2) and equating coefficients, we find a recursive set of equations for $h_n(\tilde{x}, \tilde{p})$ that are polynomials of up to order $4n$ in $\tilde{x}$ and $\tilde{p}$. This reduces the problem to solving linear equations for the coefficients. In order for the expansion (11) to be valid, $D\tilde{x}^k\tilde{p}^l$ with $k + l \leq 4$ has to be small. The above expansion thus accurately describes the center part of the PSPDF for small D. To first order, the resulting PSPDF is [33]

$$P(\tilde{x}, \tilde{p}) = \frac{e^{-\frac{\tilde{p}^2+\tilde{x}^2}{2}}}{2\pi}\left[1 + \frac{D}{4(3+4\Omega^2)}(3\tilde{p}^4 + 18\tilde{x}^2 - 27 + (4\tilde{p}^3\tilde{x} - 12\tilde{p}\,\tilde{x})\Omega + (3(\tilde{p}^2+\tilde{x}^2)^2 - 24)\Omega^2)\right]. \tag{12}$$

In practice, we perform the expansion up to order D^3; the resulting expression agrees with simulations of the PSPDF and the small-energy behavior of the marginal energy distribution $P_E(E)$ (see Fig. 1). The PSPDF has a number of interesting features. For large frequencies $\Omega \gg 1$, Eq. (12) can be expressed as a function of the Hamiltonian $H(\tilde{x}, \tilde{p}) = (\tilde{p}^2 + \tilde{x}^2)/2$, which corresponds to the underdamped limit (6). Contrary to the underdamped approximation, this small noise, small energy expansion places no restrictions on Ω, allowing us to explore the overdamped regime $\Omega \ll 1$. There, equipartition breaks down. Instead, we find that the average potential energy is larger than the kinetic one, while both the kinetic and potential energy and thus the total energy of the system increases as $\Omega \to 0$, i.e., $\omega \to 0$, see Fig. 3. This is in stark contrast to the case of linear friction, where the BG distribution factorizes into a position- and momentum-dependent part, $P_{\mathrm{BG}}(x, p) = P_x(x)P_p(p)$; the energy of the system is always equidistributed between kinetic and potential energy and the total energy is independent of the frequency. The limit $\Omega \to 0$ and the stationary limit $t \to \infty$ do not commute; we assume that the latter is taken first. Even for very low frequencies, the average kinetic energy is reduced (compared to the free particle case, dashed line in Fig. 3) by introducing the confining potential, supporting the notion that confinement increases the effectiveness of the cooling mechanism [28,33]. The breakdown of equipartition means that the temperature of the system is not uniquely defined, with different effective temperatures governing the kinetic and potential degrees of freedom.

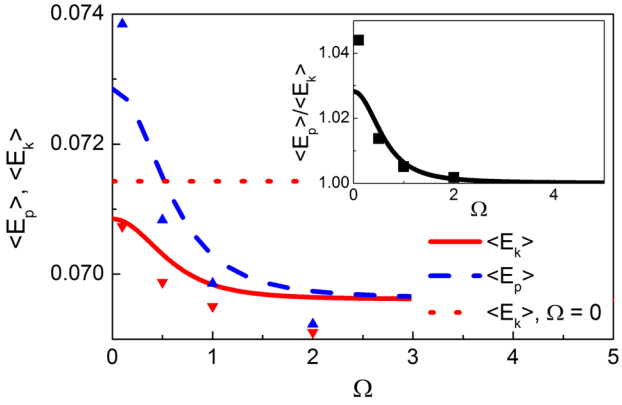

FIG. 3 (color online). Average potential and kinetic energy for $D = 0.1$ from the third-order small-D expansion as a function of trap frequency. The kinetic energy of a free particle without the potential is shown for comparison. Inset: ratio of potential and kinetic energy. For large frequencies, the energy is equally distributed between the potential and kinetic degree of freedom. For small frequencies, the potential energy is larger than the kinetic one. The symbols are the results of numerical simulations; discrepancies in the theoretical curves are due to the truncation of the expansion. Being the result of an expansion, the deviations from equipartition shown here are naturally small; however, a much larger effect can be found for larger D using numerical simulations [33].

Discussion.—We have investigated the statistical mechanics of cold atoms subject to Sisyphus cooling and a harmonic confinement in different regimes. From an experimental point of view, care needs to be taken when assigning a temperature to the particle cloud, as the latter—if interpreted in terms of kinetic energy—is generally not equal to the atoms' potential energy. In a recent experiment [14], the atoms were equilibrated with the lattice in a dipole trap, before being released in order to measure their superdiffusive motion. The trapping phase corresponds

precisely to the situation discussed in this Letter, with $\Omega \ll 1$ and $1/5 \lesssim D \lesssim 1/3$. This demonstrates that the parameter regime where the deviations from BG statistics are relevant is accessible in experiment. The condition $\Omega \ll 1$ is in fact an experimental requirement, since the semiclassical description of Sisyphus cooling breaks down when the atoms are confined on length scales of the order of the lattice wavelength [4]. For typical parameters accessible in experiments (see the Supplemental Material for details [33]), we estimate $\Omega \ll 10^{-3}$ and find sizable deviations from energy equipartition $\langle E_p \rangle \approx 3\langle E_k \rangle$ from numerical simulations. Further, our estimations show that a steady state kinetic temperature 3 times lower than the minimal value attainable for free atoms may be realized [33].

Let us come back to the questions we posed in the beginning. Is the PSPDF a function of the Hamiltonian? In the three limiting cases discussed above—namely, for large frequencies, large energies, and small D—the answer to leading order is yes. The underdamped limit, which generally requires large frequencies, also describes the large energy behavior for arbitrary frequencies and the power-law tails of the PSPDF $P(x, p) \sim [H(x, p)]^{-1/D}$ are universal. The physical reason for this is that dissipation is weak for fast particles due to the nonlinear friction force. Is the PSPDF given by BG or Tsallis statistics? Here, the answer is affirmative only for deep lattices $D \to 0$, where the PSPDF reduces to the BG result. How does the PSPDF deviate from thermostatic statistics? As the corrections to the leading order results cannot be expressed as a function of the Hamiltonian, equal energy does not imply equal probability, in contrast to thermostatic statistics [19]. The corrections lead to deviations from equipartition and lower the kinetic energy; both effects are sizable for realistic experimental parameters [33] and should be the subject of experimental study or more microscopic quantum-mechanical simulations. In summary, the steady state of confined, Sisyphus-cooled atoms is an intricate nonequilibrium state, which obeys thermostatic principles in specific limits. Beyond these limits, we find rich physics with promising applications to experiments.

This work was supported by the Israel Science Foundation.

[1] C. Tsallis, J. Stat. Phys. **52**, 479 (1988).
[2] J.-P. Bouchaud, J. Phys. I (France) **2**, 1705 (1992).
[3] F. Bardou, J. P. Bouchaud, O. Emile, A. Aspect, and C. Cohen-Tannoudji, Phys. Rev. Lett. **72**, 203 (1994).
[4] E. Lutz and F. Renzoni, Nat. Phys. **9**, 615 (2013).
[5] S. Diehl, A. Micheli, A. Kantan, B. Kraus, H. P. Büchler, and P. Zoller, Nat. Phys. **4**, 878 (2008).
[6] S. Diehl, E. Rico, M. A. Baranov, and P. Zoller, Nat. Phys. **7**, 971 (2011).
[7] M. Höning, M. Moos, and M. Fleischhauer, Phys. Rev. A **86**, 013606 (2012).
[8] C. Cohen-Tannoudji and W. D. Phillips, Phys. Today **43**, 33 (1990).
[9] Y. Castin, J. Dalibard, and C. Cohen-Tannoudji, in Proceedings of the LIKE Workshop, Marciana Marina, 1990 (ETS Editrice, Pisa, 1991), p. 5.
[10] S. Marksteiner, K. Ellinger, and P. Zoller, Phys. Rev. A **53**, 3409 (1996).
[11] H. Katori, S. Schlipf, and H. Walther, Phys. Rev. Lett. **79**, 2221 (1997).
[12] P. Douglas, S. Bergamini, and F. Renzoni, Phys. Rev. Lett. **96**, 110601 (2006).
[13] D. A. Kessler and E. Barkai, Phys. Rev. Lett. **105**, 120602 (2010).
[14] Y. Sagi, M. Brook, I. Almog, and N. Davidson, Phys. Rev. Lett. **108**, 093002 (2012).
[15] E. Lutz, Phys. Rev. A **67**, 051402 (2003).
[16] J. P. Bouchaud and A. Georges, Phys. Rep. **195**, 127 (1990).
[17] F. Bardou, J.-P. Bouchaud, A. Aspect, and C. Cohen-Tannoudji, *Lévy Statistics and Laser Cooling: How Rare Events Bring Atoms to Rest* (Cambridge University Press, Cambridge, England, 2002).
[18] R. Metzler and J. Klafter, J. Phys. A **37**, R161 (2004).
[19] A. R. Plastino and J. A. S. Lima, Phys. Lett. A **260**, 46 (1999).
[20] D. A. Kessler and E. Barkai, Phys. Rev. Lett. **108**, 230602 (2012).
[21] A. Dechant and E. Lutz, Phys. Rev. Lett. **108**, 230601 (2012).
[22] E. Barkai, E. Aghion, and D. A. Kessler, Phys. Rev. X **4**, 021036 (2014).
[23] The diffusion coefficient depends on momentum, $D_p(p)$ [9]. However, this dependence does not change the qualitative results [10].
[24] W. Greenwood, P. Pax, and P. Meystre, Phys. Rev. A **56**, 2109 (1997).
[25] Y. Castin, K. Berg-Sørensen, J. Dalibard, and K. Mølmer, Phys. Rev. A **50**, 5092 (1994).
[26] A. Dechant, E. Lutz, D. A. Kessler, and E. Barkai, Phys. Rev. E **85**, 051124 (2012).
[27] H. Risken, *The Fokker-Planck Equation* (Springer, Berlin, 1986).
[28] A. Dechant, D. A. Kessler, and E. Barkai (to be published).
[29] H. A. Kramers, Physica (Utrecht) **7**, 284 (1940).
[30] R. L. Stratonovich, *Topics in the Theory of Random Noise* (Gordon and Breach, New York, 1963).
[31] P. Hänngi, P. Talkner, and M. Borkovec, Rev. Mod. Phys. **62**, 251 (1990).
[32] M. Borkovec and B. J. Berne, J. Chem. Phys. **86**, 2444 (1987).
[33] See Supplemental Material at http://link.aps.org/supplemental/10.1103/PhysRevLett.115.173006, which contains a more detailed discussion on the various expansion procedures and some remarks on experimental parameters and includes Refs. [34,35].
[34] R. Grimm, M. Weidemüller, and Y. B. Ovchinnikov, Adv. At. Mol. Opt. Phys. **42**, 95 (2000).
[35] D. A. Steck, University of Oregon, http://steck.us/alkalidata (revision 2.1.4, 23 December 2010).